CLOSE-UP EXAMINATION OF PERFORMANCE DATA FOR A GRID-CONNECTED PV SYSTEM

Anton Driesse[1], Steve Harrison[2], and Praveen Jain[1]
[1]Department of Electrical Engineering, Queen's University, Kingston, Canada
[2] Department of Mechanical Engineering, Queen's University, Kingston, Canada

ABSTRACT

The 20-kW photovoltaic array on the facade of Goodwin Hall, Queen's University has been operating nearly continuously since July 2003 and its performance and operating conditions have been recorded in detail since that time. Analysis of the data revealed some shortcomings in the measurement process but also gave insight into different aspects of system performance, helping to identify problems and fine-tune parameters. A TRNSYS simulation model was created to serve as a basis for comparison.

1. INTRODUCTION

The 20-kW photovoltaic array on the facade of Goodwin Hall has been operating nearly continuously since July 2003. It is equipped with many additional sensors in order to characterize its operation and thereby support teaching and learning. Most PV monitoring systems record longer-term average data – perhaps hourly, daily or longer – whereas this system records changes in measured parameters with a time resolution of approximately 1 second. Additional ad-hoc instrumentation is used to capture electrical parameters with sub-second resolution.

Collecting high-resolution data presented some expected challenges, such as a high volume of data, but also some unexpected ones. The current and voltage measurements exhibit odd variations and the multiple radiation measurements are not consistent. However this is not an experiment that can be started over and it is useful to consider how this imperfect data can still yield useful information for the assessment of real-world systems.

Some aspects of system performance can be observed directly from the data, but it can also be helpful to have a model to serve as a basis of comparison. A system model was therefore built using TRNSYS 15 in order to begin investigating more complex aspects of performance.

System description

A brief description of the array and monitoring system sets the context. Figure 1 illustrates the four rows of modules mounted as awnings above the windows of the top four floors of this seven-storey building. The module slope (70° nominal) and position relative to the windows are a compromise between electrical yield and aesthetics, and also between shading, daylight and view. The 75 Wp modules are electrically connected as 12 parallel strings of 22 modules each, for a total of 264 modules and 19.8 kWp. The inverter is a Xantrex PV 20208, 20kWp, 3-phase unit connected to the grid via an isolation transformer. Further details are found on the web page dedicated to the array (2006) and in a previous publication (Driesse and Harrison, 2004).

Fig. 1 Goodwin Hall photovoltaic array

Monitoring equipment

The original objectives for monitoring of this system were dominated by the educational component, i.e. to provide an accurate portrait of a typical, operating photovoltaic installation, with data to serve as the basis for learning exercises and projects. The focus on thermal issues during the design phase (Driesse et al. 2003) highlighted the research potential and led to a proliferation of thermocouples on the façade. The electrical parameters are fewer in number and easier to capture. (See the summary in Table 1.) In addition to the custom sensors, the inverter keeps track of several parameters which are logged at 1-minute intervals and downloaded periodically, and a bi-directional energy meter completes the setup.

Table 1
Sensor summary

PARAMETER	QTY.
Solar radiation, tilted	4
Solar radiation, horizontal	1
Module temperature	12
Air temperature	18
String current	12
Array current	1
Array voltage	2
Wind speed and direction	2
Ambient temperature	1
Humidity	1
Barometric pressure	1
Total	55

2. DATA ACQUISITION CHALLENGES

Data rates and volumes

The data acquisition hardware is capable of capturing approximately one reading per second continuously and producing about 1.73 G readings per year. The archiving system uses two techniques to reduce the amount of information actually recorded. First, only changes in data that are significant (greater than the exception deviation) are reported to the database; and second, if consecutive values form nearly a straight line (based on the compression deviation) only the endpoints are stored in the database. With the deviation parameters customized for each sensor type, only about 1 in 40 readings is stored in the database on average: ranging for 1 in 1200 for temperatures (± 0.5 °C) to 1 in 13 for DC string current (± 0.02 A). When readings are extracted from the database they are interpolated as needed to reproduce the original time series within the specified tolerances. (OSIsoft, 2006)

Anomalies in voltage and current measurements

With a one-second sampling interval it was expected that all significant changes reported by the sensors would be captured and recorded accurately; that is, changes would occur with periodicities << 2 s. The grid frequency, inverter switching frequency and any harmonics would be filtered out by the data acquisition hardware. In reality, however, the DC voltage and current signals display a curious pattern that resembles a burst of oscillations repeating approximately once per minute for current (shown in figure 2) and four times per minute for the voltage, with a magnitude reaching about 5% of the average signal. To determine the source of these perturbations, we captured both voltage and current signals using digital storage oscilloscope sampling first at 1 kS/s, then at 1M S/s. Both traces show clear deviations or "blips" at half-second intervals. (See figure 3.)

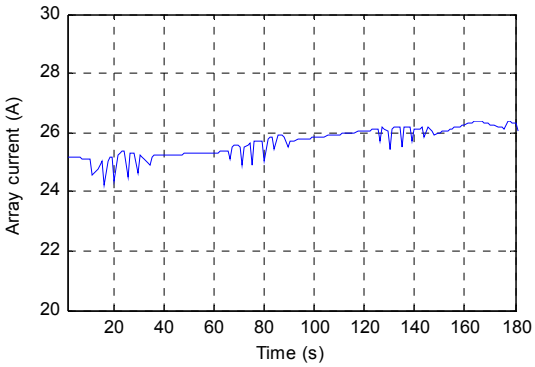

Fig. 2 Current measurements from the D/A system

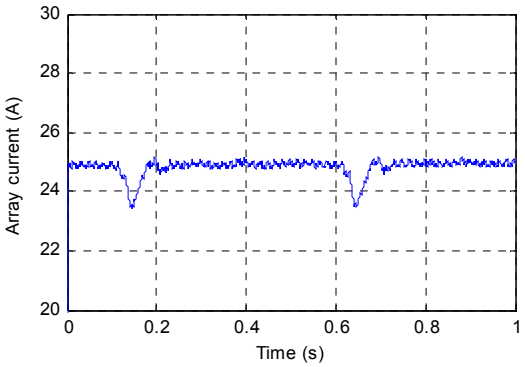

Fig. 3 Current measurements from the oscilloscope

A closer look at the signals and equipment specifications leads to an explanation. The pattern observed in the current readings repeats every 57.5 s, which corresponds to exactly 51 samples of the D/A system and exactly 115 blips in the original signal. The sampling rate of the D/A system for the voltage channels is slightly different from the current channels, so the aliasing produces a pattern that repeats every 13.5 seconds, corresponding to 11 samples of the D/A system and 27 blips in that original signal. Figure 4 illustrates how one sequence of consecutive samples of the current signal can miss the "blips", whereas a later sequence can be distorted.

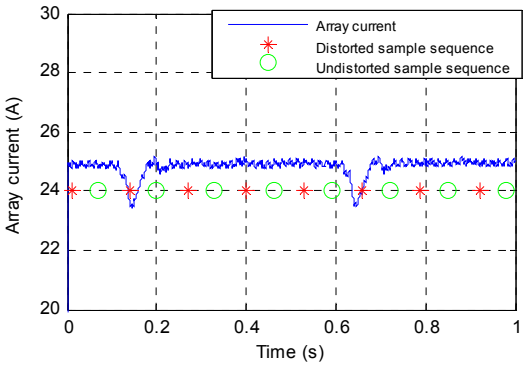

Fig. 4 Illustration of the timing for two sequences of consecutive samples relative to the "blip" pattern

Interesting as this may be, these periodic bursts nevertheless constitute an unwanted source of noise that should be filtered out. A simple method is to average the measured signals over one period, which significantly reduces the time resolution but should accurately reflect the magnitude of the original signal. Since the voltage deviations are primarily up, and the current deviations down, it is also possible to take the minimum and maximum values respectively of several consecutive samples and thereby construct a signal of samples only taken between blips. This will better show the short-term dynamics at the expense of long-term accuracy.

The root cause of the half-second deviations was identified by the manufacturer to be the active anti-islanding method, which periodically tries to shift the output current phase angle up or down.

Anomalies in radiation measurements

Four tilted pyranometers were installed – one on each level – with the objective of capturing possible differences in irradiation between the levels, as well as one horizontal one to facilitate comparison with other horizontal radiation measurements and for use in modelling. Unfortunately the data for the four tilted pyranometers appear skewed relative to each other, and while their magnitudes are comparable in winter (figure 5), the summer readings on the top level pyranometer are much lower than the others (figure 6). Although the pyranometers are out of reach, close-up photos confirm that their mounting angles are all slightly different. It appears that differences in azimuth cause the skewing of the daily profiles, and differences in slope cause the seasonal discrepancy.

Correcting or compensating the pyranometer data is a two-step process: first, the exact orientation of each sensor must be found; and second, the sensor readings must be adjusted to reflect the exact array orientation. For ideal sensors and 100% beam radiation, the adjustment factor would simply be a ratio of cosines for the angles of incidence on the array and the sensor: $\cos(\theta_{array})/\cos(\theta_{sensor})$. However, even when mounted correctly, Li-cor pyranometers are not ideal sensors. Their response varies with incidence angle (AOI), spectral content and sensor temperature, therefore published correlations (King 1997) were used to adjust all pyranometer readings based on calculated AOI and air mass (AM), and measured ambient temperature prior to making any other calculations.

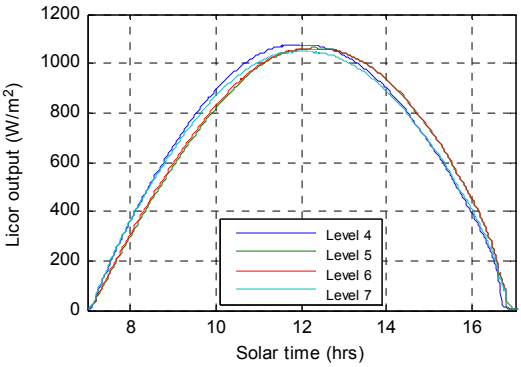

Fig. 5 Radiation readings Jan. 31, 2005

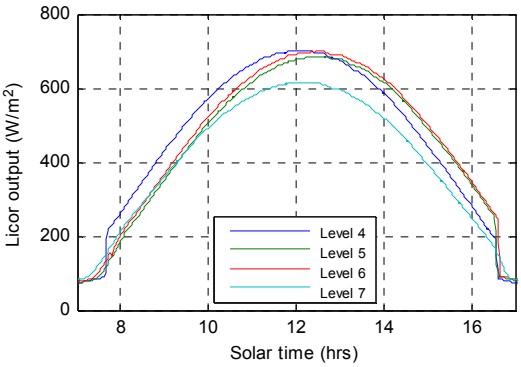

Fig. 6 Radiation readings June 27, 2005

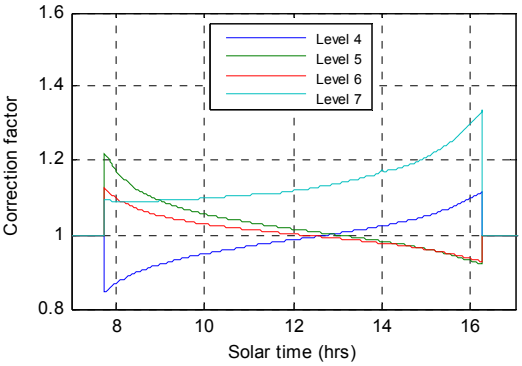

Fig. 7 Correction factors for June 27, 2005

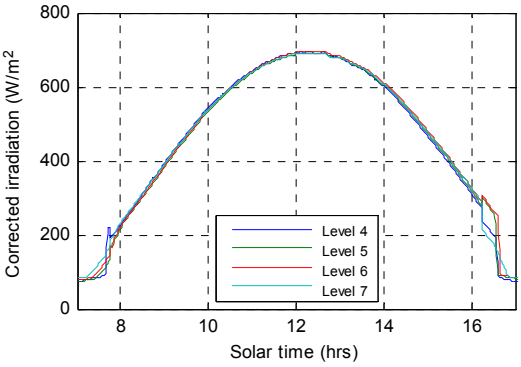

Fig. 8 Corrected readings for June 27, 2005

The photos that were taken permit a rough estimate of the sensor angles relative to the adjacent array, but this was not precise enough. Therefore, several of the clearest days in each season were chosen to compare the measured radiation profiles with the theoretical clear sky radiation on a tilted surface. The methods described by Duffie and Beckman (1991) were used first to calculate clear sky irradiation on a horizontal surface, and then the Hay-Davies anisotropic sky model was used to estimate the irradiation on a tilted surface. The calculations were automated and repeated at different surface orientations. In this manner the azimuth and slope of each sensor was deduced and the horizontal sensor was confirmed to be accurately mounted. Differences of less than half a degree were discernable in this process, and the mounting errors were much greater than that. The azimuth in particular varied by ± 4°.

The second step of adjusting sensor readings to the array orientation was accomplished by estimating the beam fraction of the total tilted radiation, and applying the cosine ratio $\cos(\theta_{array})/\cos(\theta_{sensor})$ to the beam component. (See figure 7.) It is thereby assumed that the two orientations are similar enough that the diffuse component is unaffected. The array azimuth was precisely determined by observing sunrise and sunset times relative to the façade of the building, and array slope was verified on photographic records taken during and after construction. Adjusting all four tilted sensor readings in this manner produces four nearly identical values, as shown in figure 8, supporting the validity of this process.

Despite these corrections for systemic errors, however, the fact remains that these are not the most accurate instruments, and hence two calibrated Eppley Precision Spectral Pyranometers were recently installed nearby to measure horizontal global and diffuse radiation (with a shadow band).

3. PERFORMANCE OBSERVATIONS

Inverter parameters

Several other anomalies have been noted in the data over time – things that would be hard to detect, assess, or explain without the detailed measurements at hand. During the first winter the inverter frequently shut down on sunny days because it detected too high a grid voltage, as shown in figure 9. It would then wait 6 minutes and run briefly before shutting down again. The data showed that the voltage on the inverter output terminals increased only during inverter operation, which was producing near capacity on these cold, clear days. An appropriate increase in the allowable grid voltage window made subsequent shut-downs a rarity.

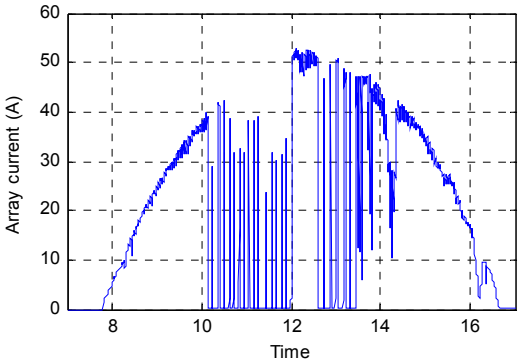

Fig. 9 Over-voltage shutdowns on Jan. 10, 2004

One hot summer day it was noticed that the inverter didn't start until 10am. (See figure 10.) The data showed that because of the heat the open circuit array voltage took a long time to reach the inverter start-up threshold voltage, and that starting times in the summer were often late. The threshold was therefore reduced and start-up times improved, but is was subsequently learned that the inverter automatically makes adjustments to this parameter as well. The accumulated data now makes it possible to gauge the effectiveness of this approach and identify circumstances that might prevent it from achieving its purpose.

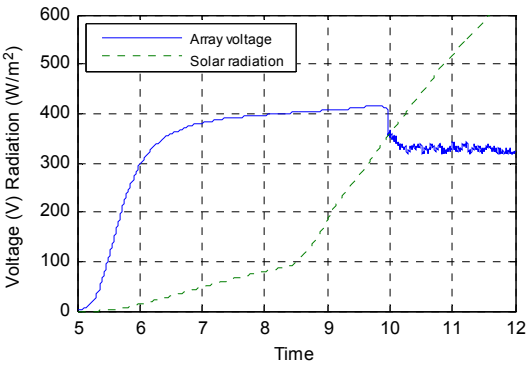

Fig. 10 Late inverter start on July 15, 2005

Module failures

Whenever the inverter is not operating, the total array current is zero, but the individual string currents are not necessarily zero because there are no blocking diodes. In fact, the strings with warmer cells and lower open circuit voltage (V_{oc}) will actually show a negative current that is offset by a positive current from the cooler strings as shown in figure 11. This effect is noticeable just before the inverter starts in the morning, but it is especially obvious when the inverter is off in the middle of a sunny day when the negative current can reach nearly one Amp.

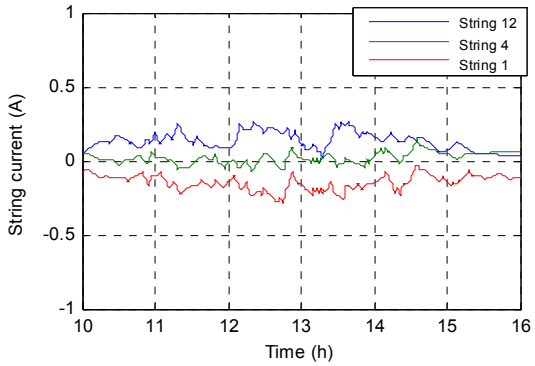

Fig. 11 String currents with inverter off, Mar. 29, 2006: upper string is coolest; lower string warmest

Strangely, there are two strings (5 and 11) whose current under open circuit conditions is always exactly zero. A possible explanation for this is that these strings have one or more modules with internal connections/contacts that have failed. Under load the string can still produce a positive current thanks to the bypass diodes in each module, but without a load the situation is different. Like the warmer strings the open circuit voltage is now too low to produce a positive current, but unlike in the warmer strings the failed connection prevents a negative current.

To test this theory, we measured the open circuit voltage on each string and found the value for string 5 to be about 10 V lower than the others. Since there is a bypass diode for every 18 cells (or half a module), a conducting diode would indeed reduce the open circuit voltage by approximately 11 V. Thus, this measurement supports the hypothesis of a failed connection on string 5.

But contrary to expectations, V_{oc} for string 11 was not significantly lower than the other strings. To investigate this further, a variable DC load was used to manually produce an I-V curve for each string. It was noted that for both strings 5 and 11, the curve showed a reduction in voltage by about 10 V at low current levels.(See figure 12.) But string 11 differs in that it produced several higher voltage readings near zero current. This evidence suggests that both strings 5 and 11 have failed connections/contacts, but whereas the failure on string 5 is complete, the one on string 11 is a very a high resistance instead.

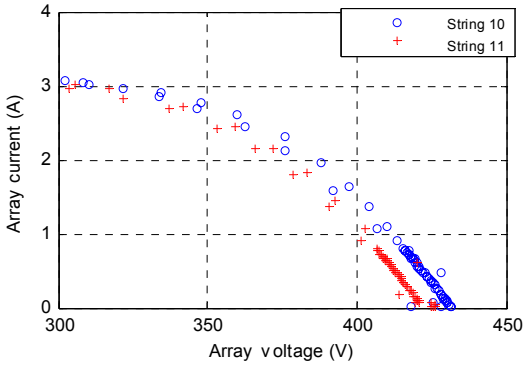

Fig. 12 I-V curves of normal string (10) and one with a defect (11)

Looking further back in the data at periods where the inverter was not operating, we find that during the first five months all strings have non-zero currents and were therefore fully functional. Later we observe segments where the current in one string is intermittently dropping to zero indicating a deteriorating connection that is making and breaking, perhaps in response to the wind gusts flexing the module. More recently a third string has begun to show the same intermittent signs of a connection failure as shown in figure 13.

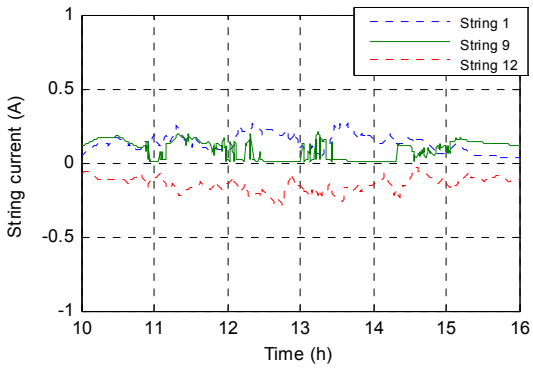

Fig. 13 Signs of intermittent failure on string 9

It is important to note that neither the V_{oc} measurements nor the I-V curves can positively identify the type of fault occurring here. They only confirm that exactly one half module is affected in each string. A shorted by-pass diode or short inside the junction box wiring would also result in a reduced string voltage similar to the connection failure; however only a connection/contact failure prevents reverse current as observed. The bypass diode has essentially become a blocking diode in this case.

Power point tracking

The blips observed in the voltage and current signals provide an interesting opportunity to test the DC operating point. A single occurrence is shown in figure 14 with current as a function of voltage, and permits us to compare the conductance (I/V) and incremental conductance (dI/dV). These should be equal in magnitude and opposite in sign at the maximum power point, yet here they are evaluated at 0.07 and -0.11 respectively, indicating that the maximum power point occurs at a lower voltage. The graph of power vs. voltage (figure 15) illustrates this more directly as the slope should be zero around the maximum power point, but is not.

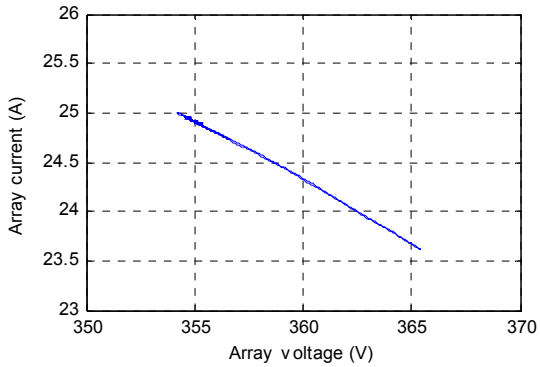

Fig. 14 Portion of the I-V curve over 500 ms.

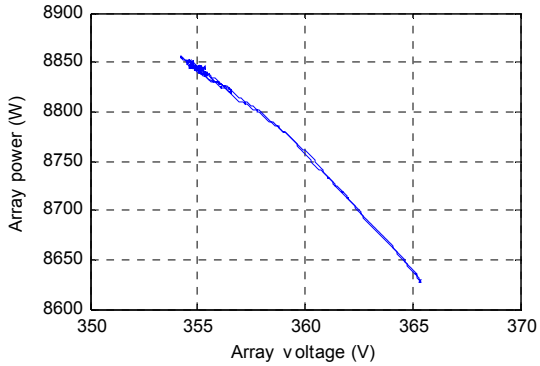

Fig. 15 Portions of the P-V curve over 500 ms.

Note however that this is one example only, and it is not meant to imply that the operating voltage is always too low. Over a longer period of time, the power point can be seen to move quite gradually around the maximum power point. Figure 16 and 17 show a period of 5 minutes during which the radiation is gradually decreasing.

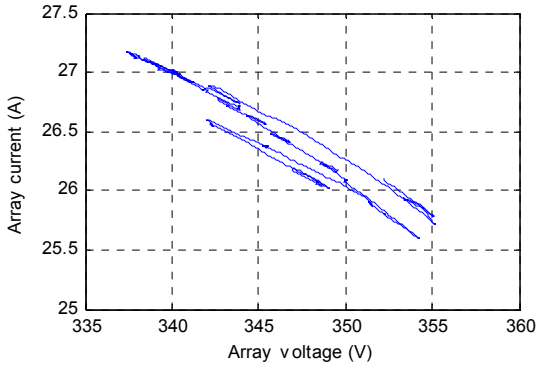

Fig. 16 Portion of the I-V curve over 5 minutes

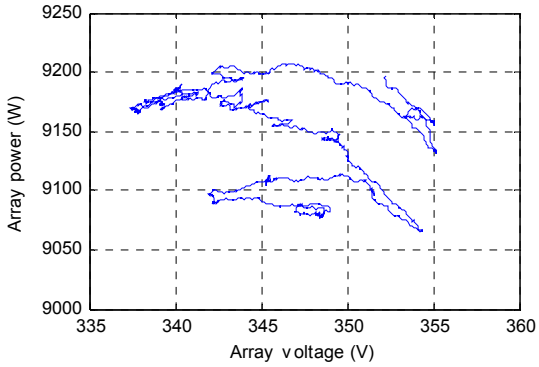

Fig. 17 Portion of the P-V curves over 5 minutes

4. MODELLING

A system model was created using TRNSYS version 15 simulation software. In its simplest form the system model is just a *data reader unit* to read the weather data, a *photovoltaic array unit* to calculate the DC electrical parameters and cell temperature, and a *printer unit* to store the results. With the appropriate inputs and outputs connected, TRNSYS can process this model for the required duration and time increment, and the output can be compared to the actual array output. A *radiation processor unit* was added to calculate the various sun angles and correct the radiation data as described in section 2. The simple model uses an array of identical cells operating under uniform operating conditions. For a more realistic representation, therefore, the array was split into 12 units – one per string – and the ambient temperatures were varied according to measurements taken on each floor. A simple shading model was also added to reduce the beam radiation to zero for certain strings based on sun angles, and 2 strings were adjusted for presumed defects.

Limitations

The TRNSYS 15 photovoltaic model includes a simple thermal model that calculates cell temperature but it does not take into account factors such as thermal mass, wind speed or building integration. Cell temperature measurements can not be used directly with this model. TRNSYS also does not provide a detailed inverter model but the array can be operated at an arbitrary voltage or MPP to simulate its interaction with the array. The time resolution for the model was set at 1/64th of 1 hour to meet TRNSYS constraints and simultaneously minimize the aliasing artefacts in the electrical measurements.

Observations and discussion

The focus of the observations using the model is on the DC operating point. One form of comparison is to consider the ideal maximum power of the array vs. the actual power output of the array; however any differences could be due to temperature, radiation, or power point tracking error. Furthermore, to actually achieve the ideal maximum power each string might have to have different operating points. Another approach is to operate the model at the measured array voltage. If the model power output then tracks that of the actual array, then the operating conditions of the model must correspond to the actual conditions. Consequently the model maximum power should be the actual maximum power and the MPP tracking error can be observed.

This comparison is illustrated for a clear day in figure 18, with a close-up in figure 19; and for a cloudy day in figure 20, with a close-up in figure 21. When the model and actual power are identical at the measured operating voltage, such as in figure 19, the model MPP should accurately reflect the actual MPP, and the MPP tracking error can be seen. When the model and actual power are not identical, such as in the left portion of figure 21, the model cell temperature and/or irradiation are incorrect and no certain conclusion can be drawn. And when all three are identical, such as in the right portion of figure 21, the model is accurate and inverter is tracking the MPP very well.

While there are segments during which the model indeed mirrors the measured power as shown, this is not consistently so. There is a strong seasonal bias as well as some difficulty in tracking rapidly changing conditions, and the simplicity of the thermal model is suspected as a major contributing factor to both since the actual module temperatures are strongly influenced by the building that supports them. Applying the model to the full dataset to draw broader conclusions is therefore not yet possible.

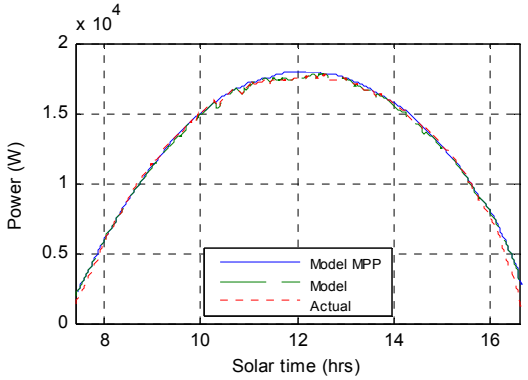

Fig. 18 Comparison of model and actual DC power levels for Jan. 31, 2005

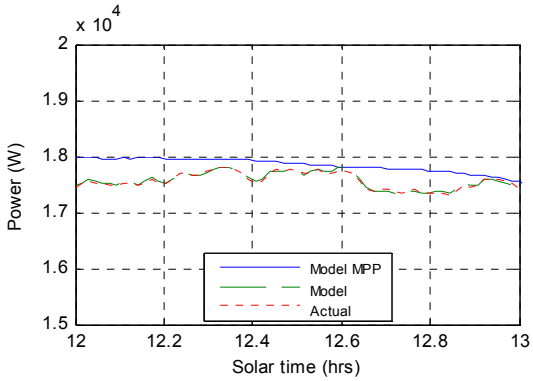

Fig. 19 Comparison of model and actual DC power levels for Jan. 31, 2005

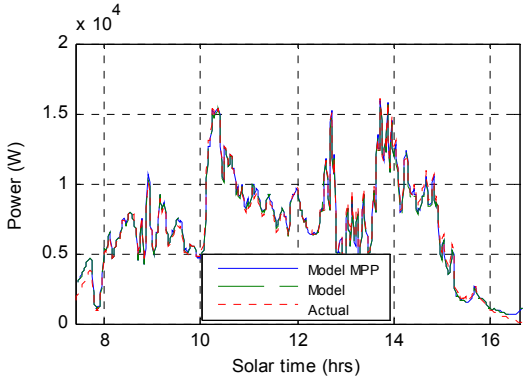

Fig. 20 Close-up of model and actual DC power levels for Jan. 29, 2005

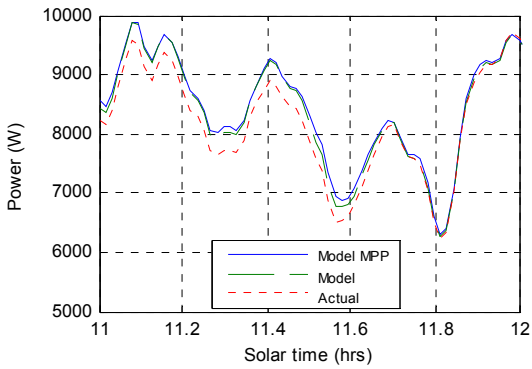

Fig. 21 Close-up of model and actual DC power levels for Jan. 29, 2005

5. CONCLUSIONS

It has been demonstrated that long-term performance data can be collected at high sampling rates and stored in a space-efficient manner while retaining significant detail. Methods were developed to compensate for shortcomings in the data collection, and these may find application in other real-world data collection projects. The data have provided direct insight into different aspects of performance, enabling inverter parameters to be adjusted, defective modules to be detected, and power point tracking to be observed. The system model developed using TRNSYS 15 provides a baseline for evaluating the array and MPPT operation, but it requires a more comprehensive thermal model in order to model the full range of conditions with consistent accuracy. After this is achieved, the inverter and transformer power conversion efficiencies should be addressed.

ACKNOWLEDGEMENTS

The authors acknowledge the financial commitment of Natural Resources Canada and Queen's University, Faculty of Applied Science for making the construction of this photovoltaic array possible. We also thank OSIsoft, Inc. for providing their data collection and analysis software and technical support at no charge.

REFERENCES

A. Driesse and S. Harrison, "Detailed monitoring and preliminary evaluation of a large façade-mounted PV array," in Proc. American Solar Energy Society Annual Conference, 2004.

A. Driesse, S. Harrison, and Q. Lin. "Analysis and Mitigation of Thermal Effects on a Large Facade-Mounted PV Array", in Proc. 2003 ISES Solar World Conference, International Solar Energy Society, 2003.

J. A. Duffie and W. A. Beckman. Solar Engineering of Thermal Processes. Wiley-Interscience, second edition, 1991.

D. L. King and D. R. Myers. "Silicon-photodiode pyranometers: Operational characteristics, historical experiences, and new calibration procedures," in Proc.IEEE Photovoltaic Specialists Conference, 1997.

PI Server Reference Guide. OSIsoft Inc., 2006.

PV array web page. appsci.queensu.ca/ilc/livebuilding/pvArray, 2006.